

Heat dissipation and acoustic emission features of titanium alloys in cyclic deformation mode

A.Yu. Iziyomova^{1,a,*}, A.N. Vshivkov^{1,b}, A.E. Prokhorov^{1,c}, I.A. Panteleev^{1,d}, V.A. Mubassarova^{1,e}, O.A. Plekhov^{1,f}, M.L. Linderov^{2,g}, D.L. Merson^{2,h}, A. Vinogradov^{3,h}

¹Institute of Continuous Media Mechanics of the Ural Branch of the Russian Academy of Sciences, 1, Ac. Koroleva str., Perm, 614013, Russia

²Institute of Advanced Technologies, Togliatti State University, 14, Belorusskaya St., Togliatti, 445667, Russia

³Department of Mechanical and Industrial Engineering, Norwegian University of Science and Technology - NTNU, 7491 Trondheim, Norway

*Corresponding author: ^afedorova@icmm.ru (<https://orcid.org/0000-0002-1769-9175>)

^bvshivkov.a@icmm.ru (<https://orcid.org/0000-0002-7667-455X>), ^cprokhorov.a@icmm.ru, ^dpia@icmm.ru, ^emubassarova.v@icmm.ru, ^fpoa@icmm.ru (<https://orcid.org/0000-0002-0378-8249>), ^gdartvi@gmail.com, ^hd.merson@iltsu.ru, ^halexei.vinogradov@ntnu.no (<https://orcid.org/0000-0001-9585-2801>)

Abstract The present work unveils the features of heat dissipation and acoustic emission accompanying the fatigue crack growth in a titanium alloy (Ti-0.8Al-0.8Mn and Ti Grade 2) using the compact tension and Charpy V-notch specimens. The quantitative measurements of the heat dissipation rate were carried out by an original heat flux sensor. The obtained results reveal that there exist two appreciably different stages of the crack propagation within the stable Paris regime. Relationships between the crack growth rate and the heat dissipation rate are proposed for both stages. The application of the non-supervised clustering algorithm to the continuously recorder acoustic emission signal helped to identify two dominant mechanisms of stress relaxation that occurs ahead of the crack tip – mechanical twinning twins and crack opening. The correlation between the acoustic emission energy and heat dissipation was found to be a harbinger of the approaching transition from stable to unstable crack growth.

Keywords Fatigue crack growth · Paris law · Heat dissipation · Acoustic emission

1 Introduction

The Paris law relating the crack growth rate da/dN to the stress intensity factor range ΔK during cyclic loading is admittedly the most popular empiric expression, which is widely used to describe the stable mode of the fatigue crack propagation in terms of the fracture mechanics: $da/dN = C\Delta K^m$ (with C and m – constants). It is widely applicable within a strong assumption of small-scale yielding conditions at the crack tip. When a plastic zone ahead of a crack tip is developed, the Paris law applies with caution considering general limitations associated with the K -concept in the linear elastic fracture mechanics. The practice-based effectiveness of this law and its extensive use in engineering does not eliminate the need to provide physically sound kinetic relations for the crack growth rate taking into account the synergistic interactions between the crack behaviour and the processes accompanying microstructural changes in the plastic zone at the crack tip.

There have been multiple suggestions for alternative functions relating the crack growth rate and the elastic-plastic fracture mechanics variables such as the J-integral, crack tip opening displacement, plastic zone size, dissipated energy, crack-size effects etc. [1-3]. For example, Carpinteri and Montagnoli [4] extended the formulation of the Paris relationship towards the short cracks with the account of crack-size effects and the associated scaling laws, using the dimensional analysis and the intermediate asymptotic theory. The energy dissipation-based approach towards the characterisation of the fatigue crack propagation behaviour has been formulated originally in [5-12].

One of the most detailed descriptions of the energy balance at the fatigue crack tip was proposed by Turner and Koledni [12]. The similar findings were reported earlier by Chudnovsky and Moet in [13] where the crack propagation law was derived as the entropy production expressed as a product of the driving force responsible for the translational mode and the corresponding thermodynamic flow in the system. Strüwe and Pippan [14] experimentally demonstrated the relationship between plastic work and the change in the stress intensity factor. Based on the thermodynamic assumption that most of this work is converted into heat, they derived the expression for the fatigue crack propagation rate. Regardless of the details, all approaches converge at that the heat dissipation is an inherent component of the energy balance at the crack tip. Thus, its quantitative assessment is pivotal for the understanding of crack behaviour. The development of a reliable technique for assessing the heat dissipation rate (or, ideally, the stored energy rate) concurrently with the fatigue crack growth rate is, therefore, indispensable. Continuous monitoring of heat dissipation is supposed to be helpful for non-destructive characterisation of different stages of crack growth and transitions between them.

In the present work, the original thermoelectric power sensor based on the Seebeck effect was developed to quantify the energy dissipation during crack propagation. Using this sensor for quantitative characterisation of the dissipated energy evolution in structural metals provides new insights and support for the concept originally formulated by J. H. Lambert in 1779 regarding the energy similitude of the mechanical and thermal failure processes in solids. This idea stems from the observation that mechanical failure of metals can occur when the relative deformation in at least one direction reaches a value equal to the linear thermal expansion at the melting point. A substantial contribution to the development of these ideas was made by V.S. Ivanova, who proposed the theory of metal fracture based on the structure-energy considerations [15]. A comprehensive analysis of the thermodynamic effects induced by cyclic deformation and fracture in metals was then carried out by Troshchenko [16] and Fedorov [17] providing an overview of the energy criteria of fracture.

The acoustic emission (AE) method has been widely applied to investigate the kinetics of the crack growth and to unveil the fracture mechanisms [18-20]. The fundamental possibility to assess the progressing damage by the energy of the AE signal has been shown by Botvina et al. in [21-23] where a relationship between AE and fracture criteria is obtained.

The correlation between the heat dissipation energy and the AE energy in concrete beams under three-point bending has been established by Carpinteri et al. [24]. These authors, in particular, have noticed that the energy releasing during the loading process is partially dissipated to create the fracture surfaces, and partially transformed into emitted energy detectable by the AE technique.

In the present work, the AE method is used to assess the fracture mechanisms through the statistical cluster analysis of AE spectral densities, and to verify the contact method proposed by the authors for estimating the heat flux in the crack tip process zone.

2 Materials and Experimental conditions

Commercially pure titanium Grade 2 and the alloy Ti-0.8Al-0.8Mn were employed in the testing program. Specimen geometries and dimensions are presented in Figure 1.

Experiments were carried out on a servo-hydraulic testing machine Instron 8802 under constant loading amplitudes of 2.5 and 3 kN at a stress ratio $R=0.1$ and loading frequency 10 Hz, using Compact Tension (CT) specimens (Fig. 1a). The crack length was measured by a clip-on crack opening displacement (COD) gauge.

The Charpy V-notch (CVN) specimens of titanium Grade 2 (Fig. 1b) with a 30-degree radius notch were tested under constant loading amplitude of 4 and 5 kN at 10 Hz frequency and $R=0$ on a 100 kN servo-hydraulic machine Bi-00-100. The crack length was measured by a potential drop method (PDM). This method is widely used to measure the crack length, detect fatigue crack initiation, visualise the surface morphology of multiple and/or branched cracks [25, 26], etc.

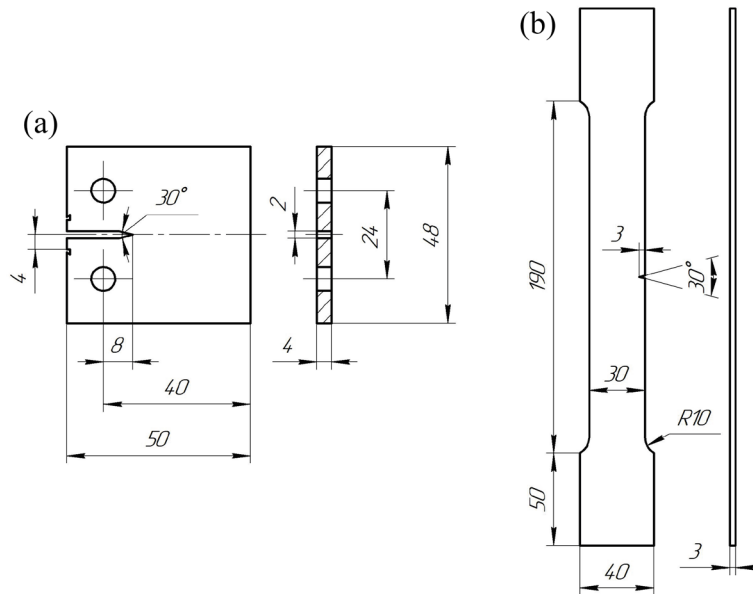


Fig. 1 Geometries of the studied titanium alloy specimens (a – Ti-0.8Al-0.8Mn and b – Ti Grade 2). All dimensions are in millimetres

The electrical potential drop crack-length-measurement technique relies on the relationship between the electrical field strength at the chosen measurement points and the geometry changes associated with a growing crack [27]. Usually, the crack length is calculated from electric-potential readings using H.H. Johnson's closed-form analytical solution. However, it is applicable for specific specimen geometries. In the present work, the PDM system was calibrated using both Johnson's formula and the experimental data obtained under conditions simulating the real test. Before testing, the correlation between the potential drop and the crack length was established for the titanium Grade 2 specimens. The calibration was performed under cyclic loading conditions. The potential drop was recorded by the NI 9205 (National Instruments) analogue-to-digital converter on the specimens with the crack length was measured by the digital optical 3D-microscope Hirox KH-7700 after each series of cycles. Figure 2 illustrates the dependence of the potential drop on the crack length for the CVN Ti Grade 2 specimens.

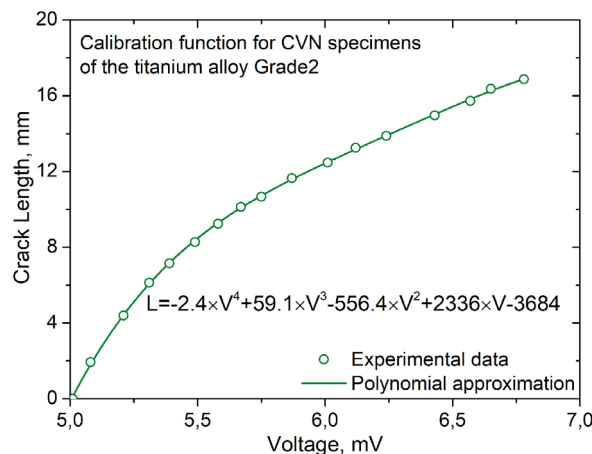


Fig. 2 Calibration curves for PDM

The quantitative measurements of the heat dissipation rate at the crack tip area were carried out using the heat flux sensor described in detail in [28]. The sensor comprises two Peltier elements and the temperature controlling feedback loop. One Peltier element is used as a heat stabiliser, while the other is used to measure the potential drop U which occurs because of the temperature difference between the plates of the Peltier element. The dependence between the potential drop in Volts and heat flux in Watts is linear. It is determined by a calibration function obtained from dedicated

calibration experiments. To provide a good thermal contact the specimen surface under heat flux gauge was coated by a thermal paste. The developed sensor can be used for direct measurements of the power of heat fluxes developing during mechanical tests of metals.

Concurrently with the heat effects, the AE signal was continuously acquired from the MSAE WB-1300 wideband (100-1300 kHz) sensor, which was securely mounted at the specimen surface in the close proximity to the notch. The 18-bit PCI-2 (MISTRAS) board was used in a thresholdless mode at 2 sample/s sampling rate. The acquisition board with triggered by timer and the AE waveforms were recorded by 10 s fragments after every 120 s of cyclic loading. The total gain was set at 60 dB in the passband of 150-1200 kHz. The adaptive sequential k-means clustering method was used to analyse the AE response [29].

3 Experimental results and data processing

Figures 3 and 4 represent the typical results for the titanium alloy Ti-0.8Al-0.8Mn and Grade 2 Ti, respectively, showing the heat flux and the crack length as a function of time; the crack growth rate is plotted versus the range of the stress intensity factor (SIF) ΔK .

Despite the differences in the testing conditions and different materials tested, the heat flux behaviour exhibits similar trends. The heat dissipation process associated with fatigue crack growth can be divided into two stages, which are coloured in Figs. 3-4 in grey and black, respectively. The first stage is characterised by the approximately constant value of the heat flux at relatively small crack lengths. The second stage is featured by the avalanche-like growth of the heat flux accompanying the rapid crack growth.

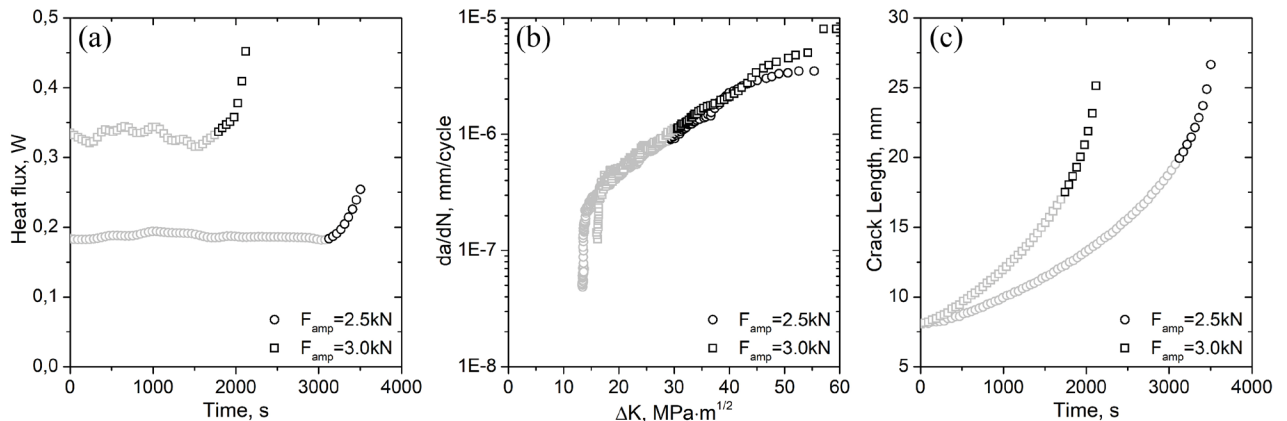


Fig. 3 Experimental data for CT specimens of the titanium alloy Ti-0.8Al-0.8Mn: a – heat flux during fatigue test; b – crack growth rate versus the SIF range; c – crack length as a function of fatigue time

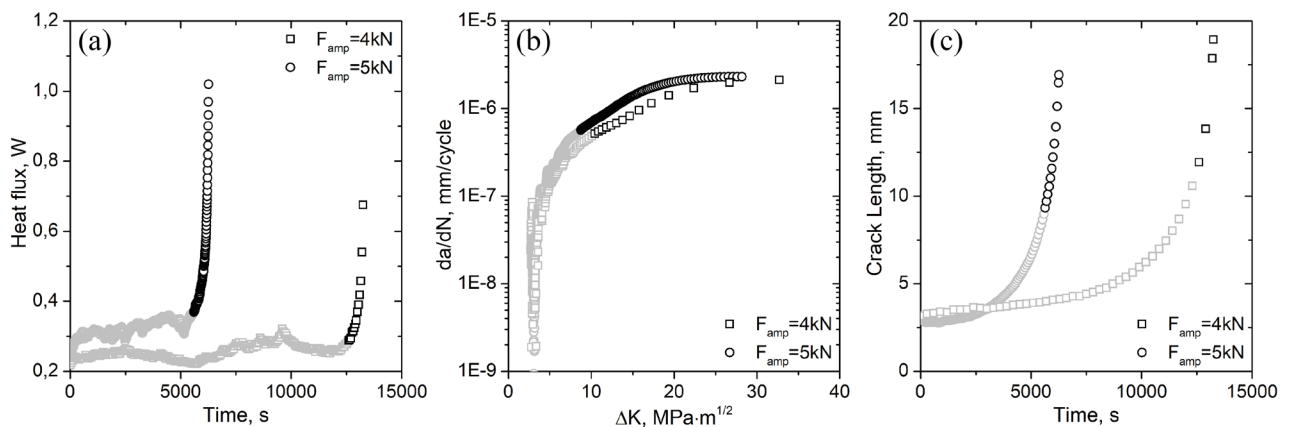


Fig. 4 Experimental data for CVN specimens of the titanium alloy Grade 2: a – heat flux during fatigue test; b – crack growth rate versus the SIF range; c – crack length as a function of fatigue time

It should be noted that significant changes in the heat flux become noticeable approximately at the middle of the linear part of the Paris curve. It can be plausibly assumed that irreversible changes in materials containing the fatigue crack start earlier than it can be envisioned from the Paris law. These changes are, however, reflected in the heat dissipation process at the crack tip.

To compare the above highlighted stages of the crack propagation, the experimental data were normalised as follows:

$$Q_1 a_1' = \frac{Q_1 a_1 - Q_1 a_1^{min}}{Q_1 a_1^{max} - Q_1 a_1^{min}}, Q_2' = \frac{Q_2 - Q_2^{min}}{Q_2^{max} - Q_2^{min}}, \Delta K_i' = \frac{\Delta K_i - \Delta K_i^{min}}{\Delta K_i^{max} - \Delta K_i^{min}}, i = 1, 2 \quad (1)$$

where Q , a and K are heat flux, crack length and stress intensity factor range, respectively. Subscript indexes correspond to the stages of heat dissipation.

The normalisation procedure (1) was applied to all experimental data with the aim at establishing the relation between the crack growth rate and the heat flux. This relation can be then compared with the Paris behaviour.

Results of data processing are presented in Figs. 5 and 6 for both materials tested, respectively. These figures demonstrate the relations between the crack growth rate da/dN and the normalised parameters $Q_1 a_1'$ and $\Delta K_1'$ (Stage 1), Q_2' and $\Delta K_2'$ (Stage 2). Figures 5c and 6c reveal that the approximately linear proportionality exists between the crack growth rate and the normalised quantities from Eq. (1).

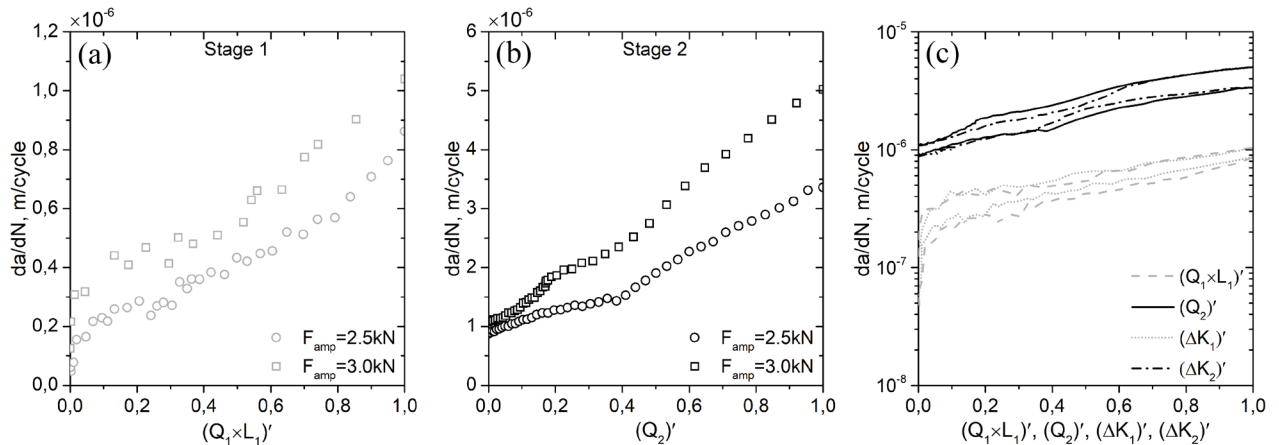


Fig. 5 The dependence of the crack growth rate on the normalised data of the heat flux and the crack length product during the first stage of the dissipation process (a) and the normalised data of the heat flux during the second stage of the heat dissipation (b); c – comparison of the normalised data with the fatigue crack growth curve (data from Ti-0.8Al-0.8Mn CT specimens)

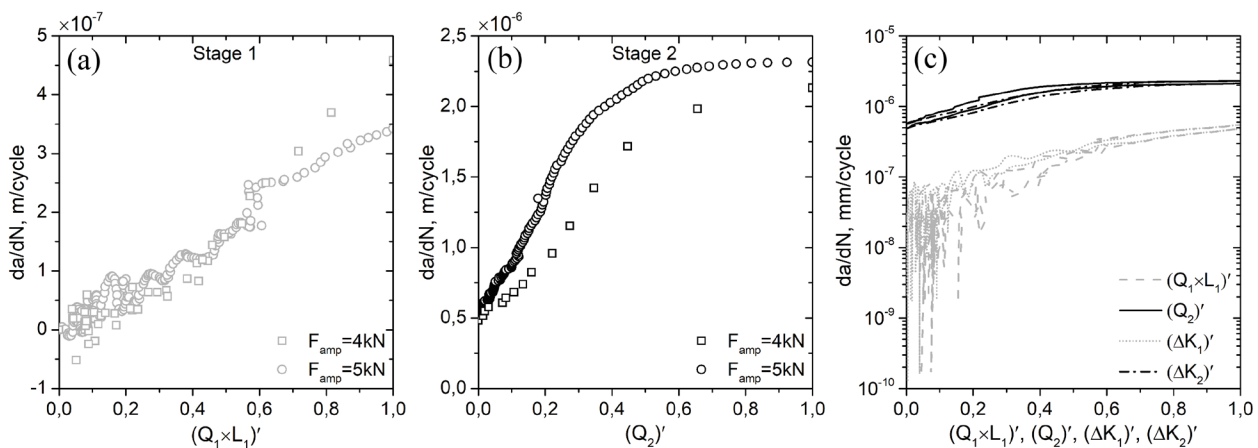


Fig. 6 The dependence between crack growth rate and normalised data of heat flux multiplied by the crack length on the first stage of dissipation process (a) and normalised data of heat flux on the second stage of heat dissipation (b); c – comparison of normalised data with fatigue crack growth curve (data from Grade 2 Ti CVN specimens).

The results presented in Figs. 5-6 exhibit linear relations for both regimes of the crack propagation. The classical Paris regime can be thus logically divided into two parts featured by different kinetics of the thermal energy dissipation. During the first stage, the crack rate is nearly linearly dependent on both the crack length and the power of the heat dissipation $\left(\frac{\partial a_1}{\partial N} \sim Q_1 a_1\right)$. The second stage is characterised by the reasonably anticipated proportionality between the crack rate and the power of the heat dissipation $\left(\frac{\partial a_2}{\partial N} \sim Q_2\right)$. The qualitatively similar result has been reported in [30], where it was shown that the knee does exist on the plot of energy required for crack propagation versus ΔK . It was proposed that the change in the specific energy corresponds to the change in the crack growth mechanism.

The AE technique powered by the spectral categorisation technique – adaptive sequential k-means clustering – revealed the presence of two stress relaxation mechanisms coexisting during the crack growth. One of these mechanisms supposedly corresponds to the nucleation of twins in the plastic zone ahead of the crack tip during crack propagation; the second is associated with the intermittent crack growth in a stop/jump manner [31, 32]. Traces of mechanical twinning are clearly visible along the crack path and the crack tip as shown in Fig. 7. One can see that the density of twins increases significantly with the crack length and the size of the plastic zone as the stress intensity increases.

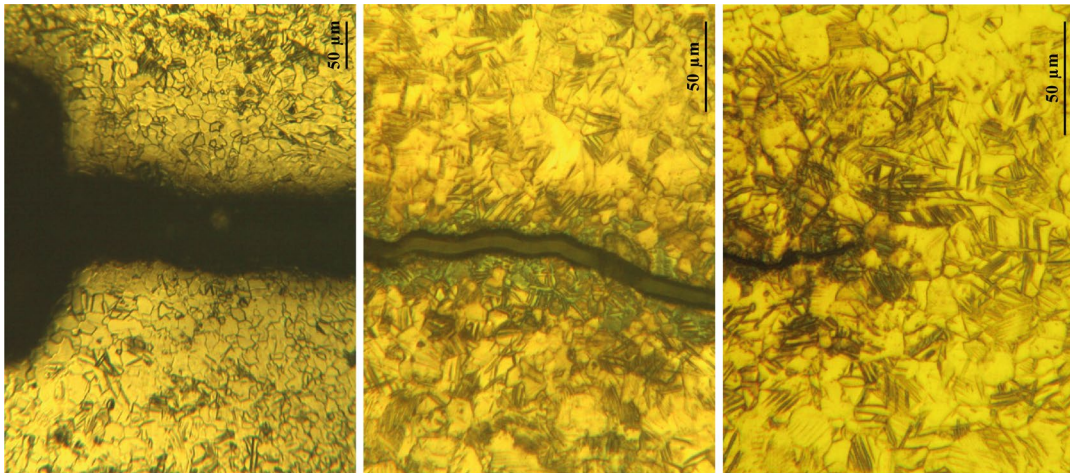


Fig. 7 The optical microscopy images showing the microstructure along the crack path in the Grade 2 Ti specimen

Figure 8 exemplifies the typical results of the AE clustering analysis. The cumulative AE energy (orange and green lines) and the heat flux (blue line) are plotted as functions of time. The decomposition of the cumulative AE energy into clusters associated with different deformation/fracture mechanisms allows establishing a correlation between the modes of the energy dissipation and the predominant type of acoustic signals accompanying the deformation and fracture processes. The orange lines in Fig. 8a-b show the time dependence of the cumulative AE energy, which was calculated for the cluster associated with the crack jumps in both materials studied. One can notice that the AE energy in this cluster accumulates nearly linearly on the early stage of the crack growth, and it grows exponentially in the avalanche-like manner at the mature stage. The transition time is marked approximately by a dashed line. The end of the linear AE stage agrees well with the time when the significant changes become appreciable in the heat flux. Thus, the two independent methods suggest that the transition between notably different stages of fatigue crack growth does exist. Concurrently, the AE signal activity associated with the second cluster, which is most likely attributable to the twin formation, becomes pronounced due to excess plasticity developing at the crack tip.

For Ti Grade 2 (Fig. 8b), the time dependence of the cumulative AE energy also can be divided into two stages. Activation of both clusters commenced approximately at the same time (of 4000 s).

The first stage is characterised by the nearly linear growth of the cumulative AE energy from 4000 s to 6000 s. The second stage (after 6000 s) is featured by the avalanche-like growth of the cumulative AE energy for both clusters. Similarly to the previous case, this moment correlates with the significant changes in the heat flux and the crack length.

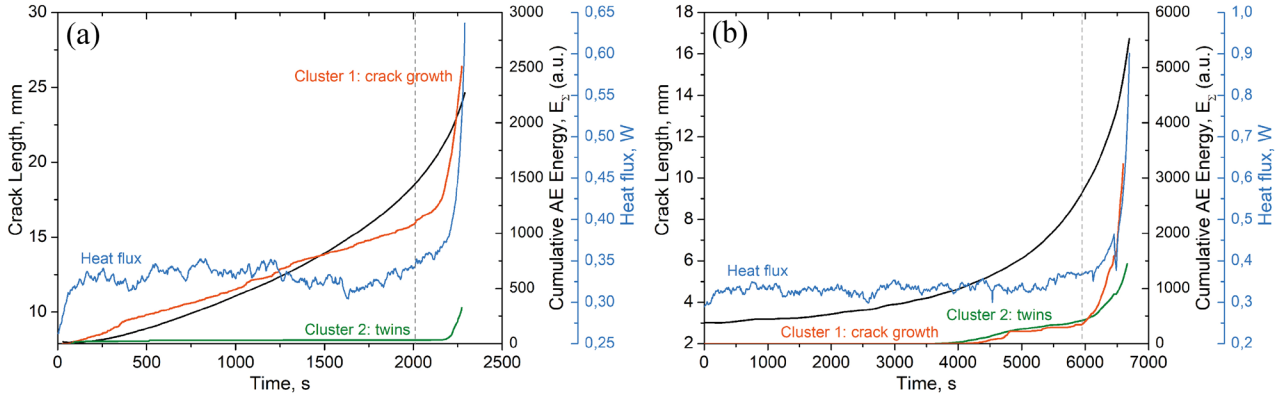


Fig. 8 Combined diagrams of the crack length (black line), heat flux (blue line) and cumulative AE energy (orange line – cluster 1 and green line – cluster 2) in time (a –Ti-0.8Al-0.8Mn, b – Ti Grade 2)

To compare the changes in the cumulative AE energy and the heat flux on the second stage of the crack growth (black line in Fig. 4), the experimental data for Ti Grade 2 were normalised as follows:

$$Q_2' = \frac{Q_2 - Q_2^{min}}{Q_2^{max} - Q_2^{min}}, \quad E_{\Sigma_2}' = \frac{E_{\Sigma_2} - E_{\Sigma_2}^{min}}{E_{\Sigma_2}^{max} - E_{\Sigma_2}^{min}}, \quad (2)$$

where Q_2 and E_{Σ_2} represent the heat flux and the cumulative AE energy on the second stage of crack propagation, respectively. A prominent result is that, once the normalisation procedure (2) was applied to experimental data, an excellent correlation was found in the behaviours of the normalised quantities - SIF, heat flux, and the cumulative AE energy in both clusters - as shown in Fig. 9.

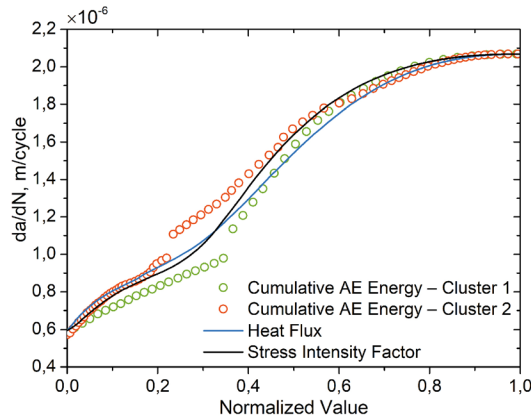


Fig.9 The dependence between the crack growth rate and the normalised data for the heat flux, cumulative AE energy and SIF corresponding to the second stage of heat dissipation (for Ti Grade 2)

Thus, one can conclude that the cumulative AE energy demonstrates the avalanche-like growth in good correlation with the heat flux during the mature stage (corresponding to the stage two of the heat dissipation) of the Paris regime of the fatigue crack growth in the materials studied. The details of this interesting relationship between these two energies – the energy dissipated by elastic acoustic waves emitting during rapid plastic deformation and fracture ahead of the growing fatigue crack and the thermal energy accompanying the same processes merit further investigations.

Let us just notice that a similar correlation was observed in [33] between the internal friction and acoustic emission measured during strain-controlled cyclic deformation of metals.

4 Conclusion

We have experimentally demonstrated that the heat dissipation at the crack tip in the Paris regime of the stable crack propagation can be divided into two stages. The first one is characterised by the constant magnitude of the heat dissipation from the crack tip. The second stage corresponds to the avalanche-like rise of the heat flux. During the first stage, the crack rate is linearly related to the product of the crack length and the power of the heat dissipation $\left(\frac{\partial a_1}{\partial N} \sim Q_1 a_1\right)$, whereas during the second stage, the crack rate is approximately proportional to the power of the heat dissipation $\left(\frac{\partial a_2}{\partial N} \sim Q_2\right)$.

The transparent physical interpretation of these results has yet to be found. However, it can be presumably associated with different mechanisms determining the crack propagation when the stress intensity factor increases. The results unequivocally show that the value of the heat flux in crack tip area reflects the energy dissipation process at the crack tip quantitatively and this paves a new way to estimate the crack growth rate independently on loading conditions.

The good correlation is established between the heat flux and the cumulative AE energy heat dissipation. The avalanche-like growth of both these properties has been observed on the mature (second) stage of the crack growth and associated with rapidly evolving plasticity at the crack tip indicating the approaching unstable crack propagation regime.

Acknowledgements. The reported study was funded by RFBR, project number 20-31-70018.

Conflict of Interest. The authors declare that they have no conflict of interest.

References

1. Iino, Y.: Fatigue crack propagation work coefficient – a material constant giving degree of resistance to fatigue crack growth. *Engineering fracture mechanics*. 12, 2, 279-299 (1979). [https://doi.org/10.1016/0013-7944\(79\)90120-6](https://doi.org/10.1016/0013-7944(79)90120-6)
2. Chow, C.L., Lu, T.J.: Cyclic J-integral in relation to fatigue crack initiation and propagation. *Engineering Fracture Mechanics*. 39, 1, 1-20 (1991). [https://doi.org/10.1016/0013-7944\(91\)90018-V](https://doi.org/10.1016/0013-7944(91)90018-V)
3. Dowling, N.E., Begley, J.A.: *Mechanics of crack growth*. ASTM STP 590. Philadelphia, PA: American Society for Testing and Materials. 83-104, 1976
4. Carpinteri, A., Montagnoli, F.: Scaling and fractality in subcritical fatigue crack growth: Crack-size effects on Paris' law and fatigue threshold. *FFEMS*. 43(4), 788-801 (2020). <https://doi.org/10.1111/ffe.13184>
5. Lindley, T.C., McCartney, L.N.: *Mechanics and mechanisms of fatigue crack growth*. *Developments in Fracture Mechanics*. Applied Science Publishers, London (1981)
6. Izumi, Y., Fine, M.E., Mura, T.: Energy considerations in fatigue crack propagation. *Int. J. Fracture*. 17, 15-25 (1981). <https://doi.org/10.1007/BF00043118>
7. Chakrabarti, A.K.: An energy-balance approach to the problem of fatigue-crack growth. *Engng Fracture Mech*. 10, 469-483 (1978). [https://doi.org/10.1016/0013-7944\(78\)90058-9](https://doi.org/10.1016/0013-7944(78)90058-9)

8. Christensen, R.M., Wu, E.M.: A theory of crack growth in viscoelastic materials. *Engng Fracture Mech.* 14, 215-225 (1981). [https://doi.org/10.1016/0013-7944\(81\)90029-1](https://doi.org/10.1016/0013-7944(81)90029-1)
9. Bodner, S.R., Davidson, D.L., Lankford, J.: A description of fatigue crack growth in terms of plastic work. *Engng Fracture Mech.* 17, 189-191 (1983). [https://doi.org/10.1016/0013-7944\(83\)90169-8](https://doi.org/10.1016/0013-7944(83)90169-8)
10. Short, J.S., Hoepfner, D.W.: A Global/local theory of fatigue crack propagation. *Engineering Fracture mechanics.* 33, 2, 175-184 (1989). [https://doi.org/10.1016/0013-7944\(89\)90022-2](https://doi.org/10.1016/0013-7944(89)90022-2)
11. Memhard, D., Brocks, W., Frick, S.: Characterisation of ductile tearing resistance by energy dissipation rate. *Fatigue Fract Engng Mater Struct.* 16, 10, 1109-1124 (1993). <https://doi.org/10.1111/j.1460-2695.1993.tb00081.x>
12. Turner, C.E., Koledni, O.: Application of energy dissipation rate arguments to stable crack growth. *Fatigue Fract Engng Mater Struct.* 17, 10, 1109-1127 (1994). <https://doi.org/10.1111/j.1460-2695.1994.tb01402.x>
13. Chudnovsky, A., Moet, A.: Thermodynamics of translational crack layer propagation. *Journal of Materials Science.* 20, 630-635 (1985). <https://doi.org/10.1007/BF01026535>
14. Strüwe, A., Pippan, R.: On the energy balance of fatigue crack growth. *Computers and Structures.* 44, ½, 13-17 (1992). [https://doi.org/10.1016/0045-7949\(92\)90218-O](https://doi.org/10.1016/0045-7949(92)90218-O)
15. Ivanova, V.S., Terentiev, V.F.: The nature of the fatigue of metals. Metallurgy, Moscow (1975)
16. Troshchenko, V.T.: Deformation and fracture of metals under high cyclic loading. Naukova Dumka, Kiev (1981)
17. Fedorov, V.V.: Thermodynamic aspects of strength and fracture of solids. FAN Uz SSR, Tashkent (1979)
18. Vshivkov, A.N., Iziumova, A.Yu., Panteleev, I.A., Ilinykh, A.V., Wildemann, V.E., Plekhov, O.A.: The study of a fatigue crack propagation in titanium Grade 2 using analysis of energy dissipation and acoustic emission data. *Engineering Fracture Mechanics.* 210, 312-319 (2019). <https://doi.org/10.1016/J.ENGFRACTMECH.2018.05.012>
19. Pascoe, J.A., Zarouchas, D.S., Alderliesten, R.C., Benedictus, R.: Using acoustic emission to understand fatigue crack growth within a single load cycle. *Engineering Fracture Mechanics.* 194, 281-300 (2018). <https://doi.org/10.1016/j.engfracmech.2018.03.012>
20. Chai, M., Zhang, J., Zhang, Z., Duan, Q., Cheng, G.: Acoustic emission studies for characterisation of fatigue crack growth in 316LN stainless steel and welds. *Applied Acoustics* 126, 101–113 (2017). <https://doi.org/10.1016/j.apacoust.2017.05.014>
21. Botvina, L.R., Soldatenkov, A.P., Tyutin, M.R., Demina, Yu.A., Levin, V.P., Petersen, T.B.: On interrelation of damage accumulation in structural steels and physical parameters estimated by methods of acoustic emission and metal magnetic memory. *Russian Metallurgy (Metally).* 2017, 10-17 (2017). <https://doi.org/10.1134/S0036029517010037>
22. Botvina, L.R., Oparina, I.B., Shebalin, P.N.: A mechanism of temporal variation of seismicity and acoustic emission prior to macrofailure. *Doklady physics.* 46, 2, 119-123 (2001). <https://doi.org/10.1134/1.1355388>
23. Botvina, L.R., Soldatenkov, A.P., Levin, V.P., Tyutin, M.R., Demina, Y.A., Petersen, T.B., Dubov, A.A., Semashko, N.A.: Assessment of mild steel damage characteristics by physical methods. *Russian metallurgy (Metally).* 2016, 1, 23-33 (2016). <https://doi.org/10.1134/S0036029516010067>
24. Carpinteri, A., Lacidogna, G., Corrado, M., Di Battista, E.: Cracking and crackling in concrete-like materials: A dynamic energy balance. *Engineering Fracture Mechanics.* 155, 130-144 (2016). <http://dx.doi.org/10.1016/j.engfracmech.2016.01.013>

25. Sato, Y., Kawaguchi, N., Ogura, N., Kitayama, T.: Automated visualisation of surface morphology of cracks by means of induced current potential drop technique. *NDT&E International*. 49, 83–89 (2012). <https://doi.org/10.1016/j.ndteint.2012.04.005>
26. Nayeb-Hashemi, H., Swet, D., Vaziri, A.: New electrical potential method for measuring crack growth in nonconductive materials. *Measurement*. 36, 121–129 (2004). <http://dx.doi.org/10.1016/j.measurement.2004.05.002>
27. Hartman, G.A., Johnson, D.A.: D-C Electric-Potential Method Applied to Thermal/Mechanical Fatigue Crack Growth. *Experimental Mechanics*. 27, 106–112 (1987). <https://doi.org/10.1007/BF02318872>
28. Vshivkov, A., Iziumova, A., Bär, U., Plekhov, O.: Experimental study of heat dissipation at the crack tip during fatigue crack propagation. *Frattura ed Integrità Strutturale*. 35, 131–137 (2016). <https://doi.org/10.3221/IGF-ESIS.35.07>
29. Pomponi, E., Vinogradov, A.: A real-time approach to acoustic emission clustering. *Mechanical Systems and Signal Processing*. 2, 791–804 (2013). <https://doi.org/10.1016/j.ymsp.2013.03.017>
30. Ranganathan, N., Chalon, F., Meo, S.: Some aspects of the energy based approach to fatigue crack propagation. *International Journal of Fatigue*. 30, 1921–1929 (2008). <https://doi.org/10.1016/j.ijfatigue.2008.01.010>
31. Vinogradov, A., Vasilev, E., Linderov, M., Merson, D.: In situ observations of the kinetics of twinning–detwinning and dislocation slip in magnesium. *Materials Science and Engineering: A*. 676, 351–360 (2016). <https://doi.org/10.1016/j.msea.2016.09.004>
32. Danyuk, A., Rastegaev, I., Pomponi, E., Linderov, M., Merson, D., Vinogradov, A.: Improving of Acoustic Emission Signal Detection for Fatigue Fracture Monitoring. *Procedia Engineering*. 176, 284–290 (2017). <https://doi.org/10.1016/j.proeng.2017.02.323>
33. Vinogradov, A., Yasnikov, I.S. On the nature of acoustic emission and internal friction during cyclic deformation of metals, *Acta Materialia*, 70, 8–18 (2014) <https://doi.org/10.1016/j.actamat.2014.02.007>